Chemistry & Biology, Vol. 10, 837–846, September, 2003, ©2003 Elsevier Science Ltd. All rights reserved. DOI 10.1016/S1074-5521(03)00192-3

Discovery of Inhibitors that Elucidate the Role of UCH-L1 Activity in the H1299 Lung Cancer Cell Line

Yichin Liu,[1,2,3] Hilal A. Lashuel,[1,2,3] Sungwoon Choi,[3,4] Xuechao Xing,[3,4] April Case,[3,4] Jake Ni,[3,4] Li-An Yeh,[3,4] Gregory D. Cuny,[3,4] Ross L. Stein,[1,2,3,4] and Peter T. Lansbury, Jr.[1,2,3,*]
[1]Center for Neurologic Diseases
Brigham and Women's Hospital
[2]Department of Neurology
Harvard Medical School
[3]Harvard Center for Neurodegeneration and Repair
[4]Laboratory for Drug Discovery in Neurodegeneration
65 Landsdowne Street
Cambridge, Massachusetts 02139

Summary

Neuronal ubiquitin C-terminal hydrolase (UCH-L1) has been linked to Parkinson's disease (PD), the progression of certain nonneuronal tumors, and neuropathic pain. Certain lung tumor-derived cell lines express UCH-L1 but it is not expressed in normal lung tissue, suggesting that this enzyme plays a role in tumor progression, either as a trigger or as a response. Small-molecule inhibitors of UCH-L1 would be helpful in distinguishing between these scenarios. By utilizing high-throughput screening (HTS) to find inhibitors and traditional medicinal chemistry to optimize their affinity and specificity, we have identified a class of isatin O-acyl oximes that selectively inhibit UCH-L1 as compared to its systemic isoform, UCH-L3. Three representatives of this class (30, 50, 51) have IC_{50} values of 0.80–0.94 μM for UCH-L1 and 17–25 μM for UCH-L3. The K_i of 30 toward UCH-L1 is 0.40 μM and inhibition is reversible, competitive, and active site directed. Two isatin oxime inhibitors increased proliferation of the H1299 lung tumor cell line but had no effect on a lung tumor line that does not express UCH-L1. Inhibition of UCH-L1 expression in the H1299 cell line using RNAi had a similar proproliferative effect, suggesting that the UCH-L1 enzymatic activity is antiproliferative and that UCH-L1 expression may be a response to tumor growth. The molecular mechanism of this response remains to be determined.

Introduction

Ubiquitin C-terminal hydrolase (UCH-L1) is one of the most abundant proteins in the brain, constituting up to 2% of total protein [1, 2]. It is normally expressed only in neurons and testis [1, 2]. UCH-L1 is a 223 amino acid cysteine hydrolase that contains the typical active site triad of cysteine, histidine, and aspartic acid [3] and catalyzes hydrolysis of C-terminal esters and amides of ubiquitin [4]. It is believed to play a key role in processing polyubiquitin and/or ubiquitylated proteolytic peptides [3–7]. An isoform of the enzyme, UCH-L3 (52% sequence identity to UCH-L1), is expressed in all tissues, including brain [1, 8]. Despite the high sequence homology, the in vitro hydrolytic activities of the two enzymes are very different; UCH-L3 is more than 200-fold more active (k_{cat}) toward a model ubiquitin amide substrate [9].

In addition to its hydrolase activity, UCH-L1 can catalyze ubiquityl transfer to a lysine residue (presumably Lys63) on another ubiquitin molecule (Figure 1A). This ligase activity requires dimerization of the enzyme [9]. UCH-L3 has little or no ligase activity as compared to UCH-L1. This ligase activity may explain why a common polymorphism of UCH-L1 (S18Y) is linked to a reduction in the risk of Parkinson's disease [10–15]. In addition to its role in PD, UCH-L1 may also play a role in the progression of certain cancers. The UCH-L1 protein is expressed in many primary lung tumors and lung tumor cell lines but is not detectable in normal lung tissue [16–21]. A positive correlation exists between UCH-L1 expression and tumor progression, suggesting that UCH-L1 may play a role in lung cancer tumorigenesis [16]. Expression of UCH-L1 also correlates with tumor progression in colorectal cancer [22]. Collectively, these data suggest that UCH-L1 is either (1) driving tumor proliferation and/or cell invasion, in which case UCH-L1 would be a potential therapeutic target for certain types of cancer, or (2) expressed in response to tumor growth.

We chose to probe the relationship of UCH-L1 and tumor progression by a forward chemical genetics approach [23, 24] starting with a screen for inhibitors of UCH-L1 enzymatic activity. The only known inhibitor of UCH-L1, the C-terminal aldehyde of ubiquitin, is not useful for studies in cell or animal models [25, 26]. We describe here a high-throughput UCH-L1 enzymatic assay, the application of that assay to screen a library of 42,000 drug-like compounds, and the optimization of the "hits" from that screen. One class of inhibitors, O-acyl oxime derivatives of isatins, demonstrated that UCH-L1 activity opposes proliferation. This class of compounds may also be useful for elucidating the etiological role of UCH-L1 in PD [9].

Results

Design of UCH-L1 HTS Screen

Both UCH-L3 and UCH-L1 catalyze the hydrolysis of ubiquitin-AMC (Ub-AMC, 7-amido-4-methylcoumarin C terminus derivative of ubiquitin) [6, 9]. Upon formation of the acyl enzyme intermediate, AMC is released from the ubiquitin C terminus (Figure 1A). The free AMC exhibits enhanced fluorescence, and the rate of AMC release was monitored by fluorescence spectroscopy (λem = 460 nm, λex = 380 nm), which was plotted against reaction time (Figure 1B). In each reaction, 300 pM of UCH-L1 was reacting with 100 nM of Ub-AMC substrate. The concentration of UCH-L1 was significantly lower than the dimerization constant (at μM range); thus, only monomeric UCH-L1 should be present [9]. In addition, since

*Correspondence: plansbury@rics.bwh.harvard.edu

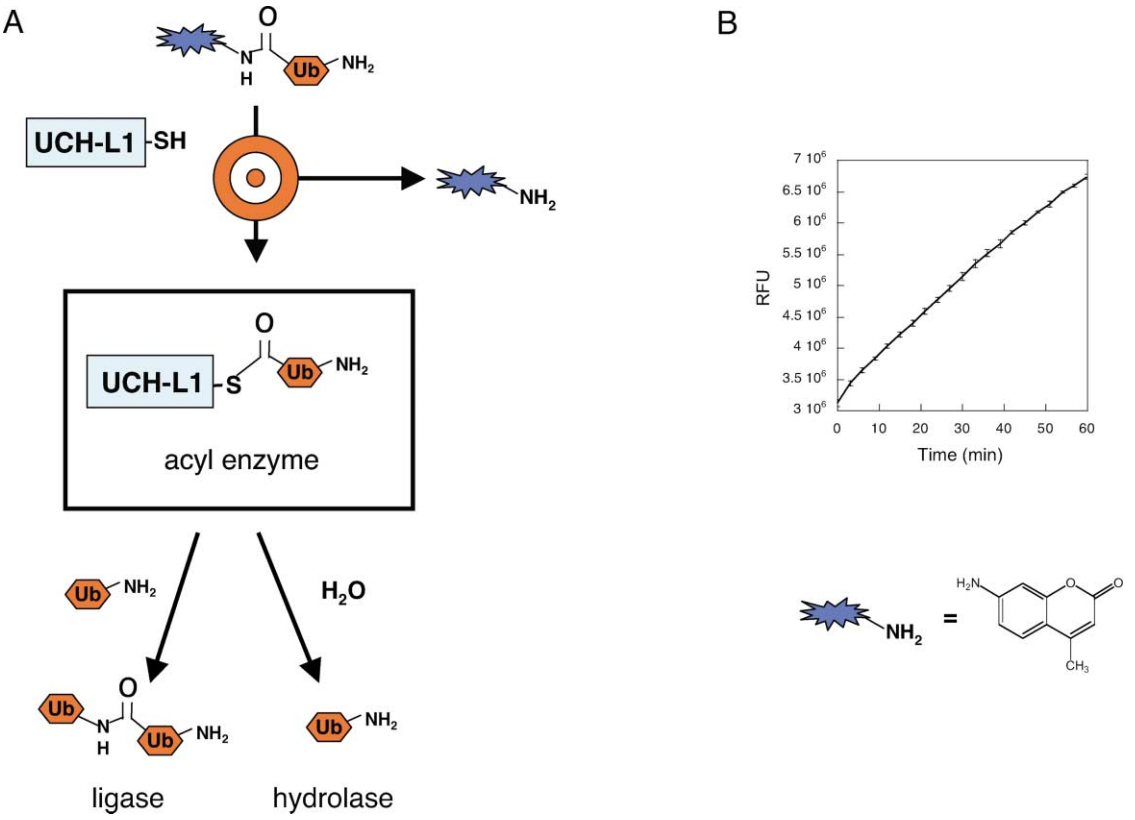

Figure 1. The High-Throughput Screen Targeted Acyl Enzyme Formation

(A) A schematic mechanism of UCH-L1 ligase and hydrolase activities, both of which proceed via acyl(ubiquityl) enzyme formation. Acyl enzyme formation was targeted by the screen described herein (see target). The rectangle is meant to signify the equilibrium mixture of monomeric and dimeric forms of UCH-L1. The dimer may be responsible for ligase activity [9].

(B) The fluorogenic substrate used (Ub-AMC) produced a fluorescent amine product, AMC (blue sunburst). The release of nonubiquitinated AMC upon acyl enzyme formation was monitored by fluorescence spectroscopy.

the reaction was run with excess substrate, multiple turnovers are observed, so the assay cannot distinguish between inhibitors of ubiquityl enzyme formation and inhibitors of ubiquityl enzyme breakdown (subsequent data presented below strongly suggest that our hits are active site directed and thus probably inhibit the former step). The identification of specific inhibitors for UCH-L1 acyl enzyme formation was accomplished by screening compound libraries for their ability to inhibit enzyme-mediated cleavage of the AMC fluorophore from ubiquitin-AMC. A minimum reaction time of 30 min was required to screen 3000 compounds. The concentration of UCH-L1 and its substrate Ub-AMC were optimized for the HTS to yield a linear velocity of AMC release over a period of at least half an hour (Figure 1B), and thus the decrease in AMC fluorescence emission observed after quenching of the reaction correlates to enzyme inhibition. The Z' factor, a standard statistical parameter for HTS assays that is reflective of both the assay signal dynamic range and the data variation associated with the signal measurements, was determined to be 0.61 ($n = 51$ for both positive and negative controls in three separate 384-well plates), indicative of a robust HTS assay (>0.5) [27].

The screening library consisted of 42,000 compounds that, in general, had the following characteristics [28]: (1) molecular weights less than 600 D, (2) log P less than 5, (3) fewer than 5 H bond donors, and (4) fewer than 10 H bond acceptors. From the primary robot-assisted screen, 1% of the compounds showed inhibitory activity (>60%) toward UCH-L1. About two-thirds of these compounds were eliminated after repeated manual analysis (secondary screen, see Experimental Procedures). Finally, only those compounds that showed dose-dependent inhibition of UCH-L1 and did not interfere with AMC fluorescence were subjected to IC_{50} determination against UCH-L1 and/or UCH-L3 (see Experimental Procedures).

Compounds from the Libraries Showed Various Degrees of Inhibitory Activity toward UCH-L1

Among the compounds that emerged from the screening process, a set of oxime derivatives of isatin (1–8) demonstrated micromolar IC_{50} values toward UCH-L1 and a consistent preference for UCH-L1 over UCH-L3 (Figure 2A). Molecules of this class, albeit not these specific acyl oximes, have previously been reported to have antitelomerase activity [29], ion channel-activating activity [30], antagonism of excitatory amino acids [31], and inhibitory activity for c-Jun N-terminal kinase (JNK) [32]. During the screening process, some inhibitors were found to be selective for UCH-L3 over UCH-L1 (Figure

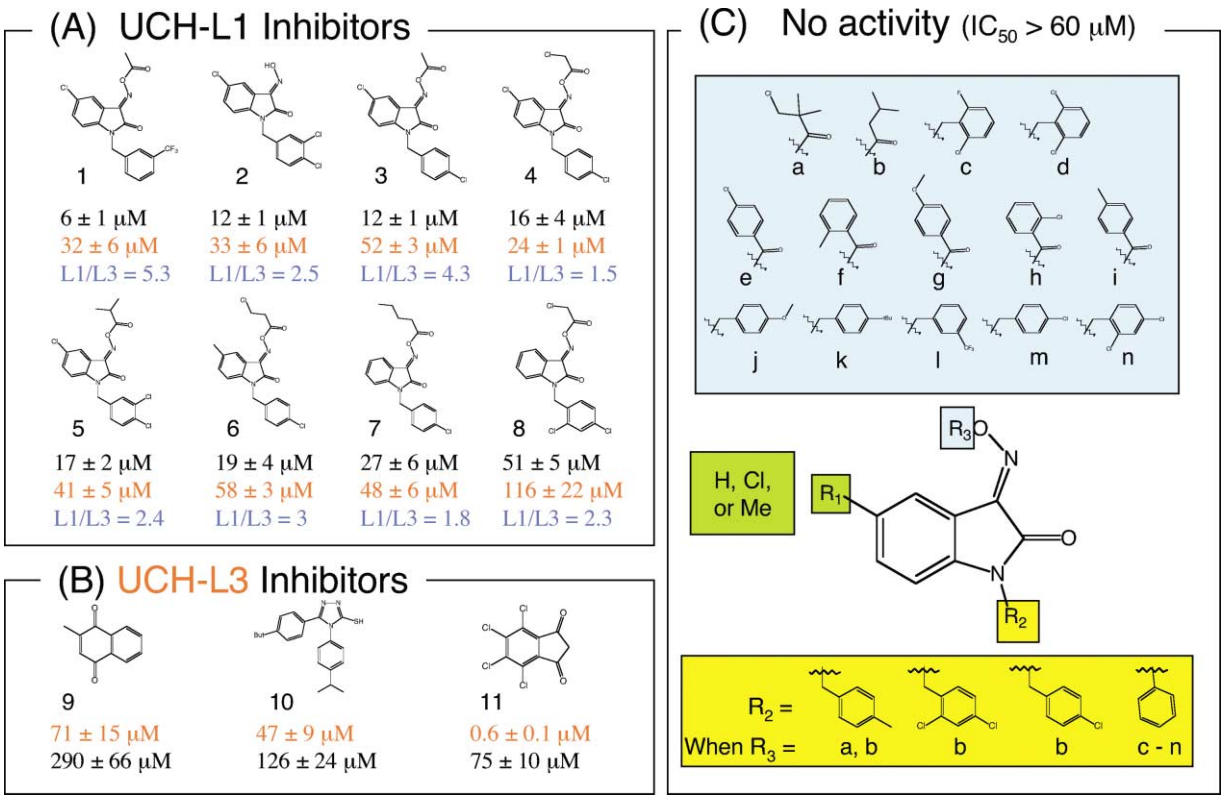

Figure 2. Inhibitory Activities of the Compounds from the Initial Library

(A) A series of isatins from the initial library (**1–8**) showed inhibitory activity and selectivity for UCH-L1 over UCH-L3. A more detailed analysis showed that these compounds have IC_{50} values for UCH-L1 ranging from 6 to 50 μM with as much as a 5-fold selectivity for UCH-L1 (IC_{50} values indicated in black) over UCH-L3 (IC_{50} values indicated in red).

(B) Three compounds showed selectivity for UCH-L3 over UCH-L1. These compounds, menadione **9** (commonly known as vitamin K_3), **10**, and **11**, were selective for UCH-L3 (IC_{50} values indicated in red) over UCH-L1 (IC_{50} values indicated in black) by as much as 100-fold.

(C) A list of isatin derivatives that have IC_{50} values for UCH-L1 greater than 60 μM. Note that only compounds with the indicated combinations of R_3 and R_2 were in the library. Wavy lines bisect bonds to atoms indicated in central structure.

2B). These compounds included menadione **9** (vitamin K_3), **10**, and **11**, the latter of which is selective for UCH-L3 over UCH-L1 by over 100-fold.

Structure-Activity Relationship Derived from Analysis of Isatin Derivatives

Eight isatin oximes (**1–8**) from the primary screen passed the rigorous validation assays and were selective for UCH-L1. A more detailed analysis showed that this class of compounds had IC_{50} values for UCH-L1 ranging from 6 μM to 51 μM with as much as 5-fold selectivity for UCH-L1 over UCH-L3 (Figure 2A). The screening library also contained a subset of oxime isatins that had no effect on UCH-L1 hydrolase activity (Figure 2C). Several general trends can be drawn from these two sets of compounds with respect to their ability to inhibit UCH-L1. First, increasing the size of the substituent on R_3 resulted in decreased activity (Figures 2A and 2C). Neither long hydrocarbon chains nor bulky phenyl rings yielded good inhibitors. Second, the phenyl substituent at the R_2 position appeared to require a linker of at least one carbon. All of the compounds that lacked such a linker were inactive, although the absence of activity may be partially due to the large R_3 substituents. Finally, the benzo portion of the isatin ring tolerated a variety of substituents (R_1).

Continued Analysis of Isatin Oxime Structure-Activity Relationship for UCH-L1 Inhibitory Activity

Oxime and O-acyl oxime derivatives of isatins were prepared according to the following method (Supplemental Figure S1 at http://www.chembiol.com/cgi/content/full/10/9/837/DC1). First, the isatins were deprotonated with sodium hydride in DMF and then alkylated with various benzyl or 2-phenethyl bromides to yield N-alkylated isatins. Next, these compounds were converted to their corresponding oximes by treatment with hydroxylamine hydrochloride in methanol:THF (1:1) and the presence of NaOAc at room temperature. Finally, O-acylation was accomplished either with an acid chloride or an anhydride in dichloromethane in the presence of pyridine (and in some cases 4-N, N-dimethylaminopyridine) to give the O-acyl oxime isatin derivatives. The compounds prepared for in vitro enzymatic activity evaluation are shown in Tables 1 and 2.

The structure-activity relationship study was conducted in order to increase UCH-L1 inhibitory potency and selectivity for UCH-L1 over UCH-L3. First, the data

Table 1. Comparison of the UCH-L1 Inhibitory Activity for Acylated Oxime Isatin Derivatives versus Nonacylated Oximes

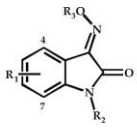

Cpd No.	R_1	R_2	R_3	UCH-L1 IC_{50} (μM)	Cpd No.	R_3	UCH-L1 IC_{50} (μM)	IC_{50} Acyl-Oxime / IC_{50} Oxime
12	5-Cl	CH_2-3,4-di-Cl-Ph	$COCH_3$	1.8	21	H	12	6.7
13	5-Cl	$CH(CH_3)$-3-CF_3-Ph	$COCH_3$	3.4	22	H	22	6.5
14	5-OCF_3	CH_2-3-CF_3-Ph	$COCH_3$	3.4	23	H	78	23
15	5-Cl	CH_2CH_2-3-CF_3-Ph	$COCH_3$	4.1	24	H	80	20
16	5-F	CH_2-3-CF_3-Ph	$COCH_3$	6.1	25	H	43	7.0
17	5-Cl	$CH(CH_3)$-2-CF_3-Ph	$COCH_3$	8.8	26	H	45	5.1
18	5-Cl	CH_2-4-CF_3-Ph	$COCH_3$	12	27	H	13	1.1
19	5-Cl	CH_2-2-CF_3-Ph	$COCH_3$	18	28	H	321	18
20	5-Cl	CH_2-3-CF_3-Ph	$COCH_3$	36	29	H	114	3.2

Acylated oxime isatin derivatives are shown in blue and nonacylated oximes are shown in red.

shown in Table 1 suggested that acylation of the oxime group is critical for increasing potency toward UCH-L1, but a similar increase in activity was not observed in the case of UCH-L3 (data not shown). For example, compound **21** has an IC_{50} value of 12 μM and its acylated derivative **12** has an IC_{50} value of 1.8 μM for UCH-L1 inhibition, a 6.7-fold increase in activity. In contrast, IC_{50} values for UCH-L3 inhibition for **21** and **12** were 33 μM and 40 μM, respectively, suggesting that the acyl group was not critical for UCH-L3 activity. In the most pronounced case (**14** versus **23**), the acylated oxime resulted in a 23-fold increase in activity toward UCH-L1 compared to the oxime.

Table 2. IC_{50} Values of O-Acyl Oxime Isatin Derivatives

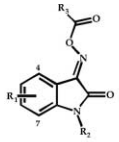

Cpd No.	R_1	R_2	R_3	UCH-L1 IC_{50} (μM)	UCH-L3 IC_{50} (μM)	L1/L3
30	5-Cl	CH_2-2,5-di-Cl-Ph	Me	0.88	25	28
31	5-Cl	CH_2-2,4-di-Cl-Ph	Me	1.2	25	21
32	5-Cl	CH_2CH_2-3,4-di-Cl-Ph	Me	1.3	22	17
33	5-Cl	CH_2-3,5-di-Cl-Ph	Me	1.3		
34	5-Cl	CH_2-3,4-di-Cl-Ph	Me	1.8	40	22
35	5-Cl	CH_2-2,3-di-Cl-Ph	Me	2.7		
13	5-Cl	CH(Me)-3-CF_3-Ph	Me	3.4	47	14
15	5-Cl	CH_2CH_2-3-CF_3-Ph	Me	4.1	113	28
1	5-Cl	CH_2-3-CF_3-Ph	Me	6	32	5
36	5-Cl	CH_2CH_2O-3-4-di-Cl-Ph	Me	6.2		
37	5-Cl	CH_2-2-Cl-5-F-Ph	Me	6.5		
17	5-Cl	CH(Me)-2-CF_3-Ph	Me	8.8		
38	5-Cl	CH_2CH(Br)-3-CF_3-Ph	Me	9.5		
3	5-Cl	CH_2-4-Cl-Ph	Me	12	52	4
18	5-Cl	CH_2-4-CF_3-Ph	Me	12		
39	5-Cl	CH_2-3-OMe-Ph	Me	13		
40	5-Cl	CH_2-2-naphthyl	Me	14		
41	5-Cl	$CH_2CH_2CH_2$-3,4-di-Cl-Ph	Me	16		
19	5-Cl	CH_2-2-CF_3-Ph	Me	18		
42	5-Cl	CH_2CH(OH)-3-CF_3-Ph	Me	19		
43	5-Cl	CH_2CH_2Ph	Me	19		
44	5-Cl	CH_2-3-Cl-4-OMe-Ph	Me	21		
45	5-Cl	CH_2-4-OMe-Ph	Me	52		
46	5-Cl	CH_2CH(OAc)-3-CF_3-Ph	Me	95		
47	5-Cl	CH_2-3-pyridyl	Me	>100		
48	5-Cl	CH_2-4-pyridyl	Me	>100		
49	5-Cl	CH_2-Ph-4-CO_2H	Me	>100		
50	5-Br	CH_2-3,4-di-Cl-Ph	Me	0.81	17	21
51	5-I	CH_2-3,4-di-Cl-Ph	Me	0.94	23	24
12	5-Cl	CH_2-3,4-di-Cl-Ph	Me	1.8	40	22
52	5-CO_2Me	CH_2-3,4-di-Cl-Ph	Me	2.6	16	6
53	5-OMe	CH_2-3,4-di-Cl-Ph	Me	2.9	18	6
14	5-OCF_3	CH_2-3-CF_3-Ph	Me	3.4	72	21
54	5-$CONH_2$	CH_2-3,4-di-Cl-Ph	Me	4.1		
55	6-Cl	CH_2-3-CF_3-Ph	Me	5.8		
1	5-Cl	CH_2-3-CF_3-Ph	Me	6	32	5
16	5-F	CH_2-3-CF_3-Ph	Me	6.1		
56	5-Ph-4-OMe	CH_2-3,4-di-Cl-Ph	Me	6.1		
57	5-Cl, 7-Me	CH_2-3-CF_3-Ph	Me	12		
58	5-CN	CH_2-3,4-di-Cl-Ph	Me	12		
59	5-SO_2NH_2	CH_2-3,4-di-Cl-Ph	Me	12		
60	5-SO_2NHAc	CH_2-3,4-di-Cl-Ph	Me	15		
61	5-I	CH_2-3,4-di-Cl-Ph	CH_2OMe	16		
62	5-C≡C-tBu	CH_2-3,4-di-Cl-Ph	Me	16		
5	5-Cl	CH_2-3,4-di-Cl-Ph	i-Pr	17	41	2.4
20	4-Cl	CH_2-3-CF_3-Ph	Me	36		
63	5-CO_2H	CH_2-3,4-di-Cl-Ph	Me	50		

Several conclusions can be drawn concerning inhibition of UCH-L1 by O-acyl oxime isatins (Table 2). A tether length of one or two carbons between the heterocyclic core and R_2 is optimal. A tether length of zero (see primary library screening data, Figure 2C) and three atoms (e.g., **36** and **41**) resulted in diminished activity. Some additional substitution of the tethering chain was permitted (e.g., **13**). However, other substituents were detrimental (e.g., **38**, **42**, and **46**) to activity. Electron-withdrawing groups in the 3- and 4-positions of R_2 (e.g., **1** and **18**) were preferred over the 2-position (e.g., **19**), but disubstituted rings having one of the substituents at the 2-position were tolerated (e.g., **30** and **31**). Likewise, small electron-withdrawing groups (R_1) in the 5- and 6-positions of the heterocyclic core (e.g., **50**, **51**, **52**, **55**, and **14**) led to greater activity. Substitution at the heterocyclic ring's 4-position was not tolerated (e.g., **20**). Only small, unbranched alkyl groups (e.g., methyl) were permitted at the R_3 position. Both long unbranched and small branched alkyl groups were not tolerated. These O-acyl oxime isatins are soluble in aqueous solution with neutral pH, although small crystals of compounds were observed at concentration of 5 μM in protein buffer after 1 hr of incubation at room temperature. A summary of the structure-activity relationship and the structures of the three most potent inhibitors (**30**, **50**, and **51**) are shown in Figure 3A.

As the potency toward UCH-L1 increased, the specificity was also improved (Table 2). The two best cases tested were **30** and **51**, which favored UCH-L1 over UCH-L3 by 28- and 24-fold, respectively (Figure 3B). Both compounds had submicromolar IC_{50} values for UCH-L1 hydrolase activity. The widening gap between the compounds' activities toward UCH-L1 and UCH-L3 resulted from an increase in UCH-L1 inhibitory activity, with little or no change in UCH-L3 inhibitory activity.

Several other changes to the O-acyl oximes were made to further explore the structure-activity relationship (Figure 3C) for UCH-L1 inhibition. For example, isatin derivatives **68** and **69** were not capable of inhibiting UCH-L1 enzymatic activity at the concentration tested (100 μM). Likewise, carbamate **64** and the acetyl hydrazones **65** and **66** were prepared. In all cases the UCH-L1 inhibitory activity was diminished ($IC_{50} > 40$ μM). O-alkyl oxime **67** also had lower UCH-L1 inhibitory activity, further supporting the importance of the O-acyl oxime group for activity.

O-Acyl Oxime Compounds Are Reversible Competitive Inhibitors of UCH-L1

Several experiments were performed to characterize the inhibitory mechanism of the O-acyl oximes. Various amounts of Ub-AMC were titrated against 1 nM UCH-L1 in the presence of different concentrations of **30**. The resulting Michaelis-Menten plot showed an increase in $K_{M,app}$ without affecting the $k_{cat,app}$ of the UCH-L1/Ub-AMC

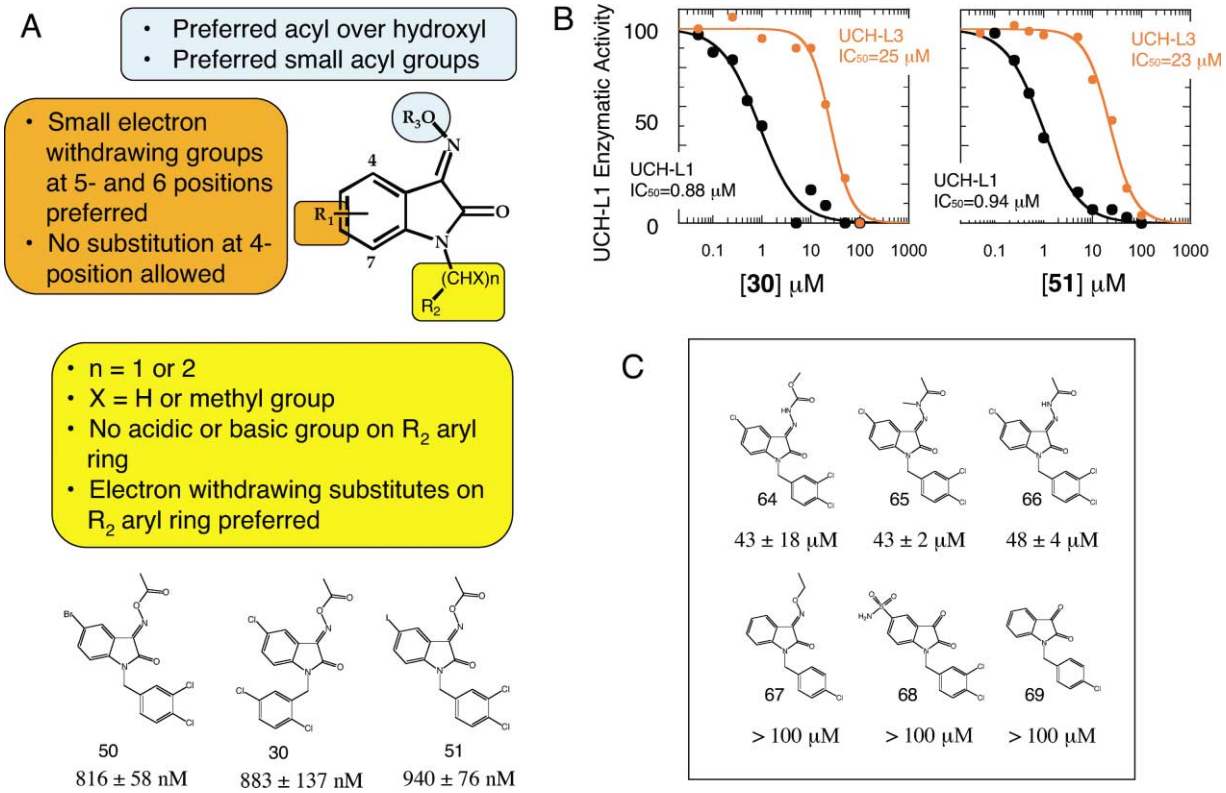

Figure 3. The Inhibitory Activity and Specificity of the Isatin Oxime Derivatives

(A) UCH-L1 inhibition structure-activity relationship summary for isatin oxime derivatives. Three potent inhibitors, **30**, **50**, and **51**, are shown at bottom.

(B) Compounds **30** and **51** show a strong preference for UCH-L1 over UCH-L3. IC_{50} curves of UCH-L1 (black) and UCH-L3 (red) for **30** and **51**.

(C) Compounds related to **30** and **51** that showed a significant decrease in inhibitory activity toward UCH-L1 ($IC_{50} > 40$ μM).

reaction (Figures 4A and 4B). This result suggested that **30** is a competitive and reversible inhibitor of UCH-L1. The linear fit of $K_{M,app}$ on [**30**] plot yielded a K_i value of 0.40 μM (Figure 4C). This K_i is consistent with the value (0.48 μM) predicted from its IC_{50} (0.88 μM) determined in separate experiments (Table 2), using the following relationship for competitive inhibition (equation 1):

$$K_i = \frac{IC_{50}}{1 + \frac{[Ub - AMC]}{K_M}}, \quad (1)$$

where [Ub-AMC] = 50 nM and the K_M for the UCH-L1/Ub-AMC reaction was 59 nM (Figure 4C). The average $k_{cat,app}$ was 0.049 ± 0.006 s^{-1} (Figure 4B) and is in agreement with previous published data [9].

To determine if the isatin O-acyl oximes are binding at UCH-L1's active site, different concentrations of **30** were added to the UCH-L1/Ub-AMC reaction in the presence of a thiol alkylating agent. For example, in the presence of 20 mM iodoacetamide, UCH-L1 loses enzymatic activity, presumably by derivitization and inactivation of the active site cysteine (Figure 4D). When increasing amounts of **30** were added to the reaction mixture, the rate of UCH-L1 inactivation by the alkylating reagent was decreased (Figure 4E). This result indicated that binding of the isatin O-acyl oxime protected the UCH-L1 active site cysteine, supporting the hypothesis that these inhibitors occupy the enzyme active site. Finally, thin-layer chromatography (TLC) and ^{1}H NMR analyses of the reaction mixtures containing **30** or **14** (with or without UCH-L1) after 2 hr of incubation showed no change in the compounds' composition (data not shown), demonstrating that they are stable in aqueous buffer and are not chemically altered by UCH-L1.

O-Acyl Oxime Compounds Promote Proliferation of H1299 and SH-SY5Y Cells

To test the effect of UCH-L1 inhibitors in a cell culture model, H1299 (an UCH-L1-expressing non-small cell lung cancer [NSCLC]) and H358 (a NSCLC line that does not express UCH-L1) (Figure 5A) [19] were treated with 5 μM of **15**, **30**, **50**, or **52**. As negative controls, the cells were also treated with 5 μM of **24** (a relatively inactive derivative: IC_{50} = 80 μM) and pure DMSO. Cell growth was quantified by counting the number of living cells as a function of time. The concentration of 5 μM was chosen because it is 2-fold or higher than the IC_{50}s of compounds **30**, **50**, and **52** toward UCH-L1, yet it is significantly lower than all the compounds' IC_{50}s toward UCH-L3. The cell counts of both the H358 (Figure 5C) and H1299 (Figure 5B) lines increased by comparable amounts when treated with DMSO or **24**. Two of the potent compounds, **50** and **52**, dramatically increased proliferation of H1299 cells (none affected proliferation

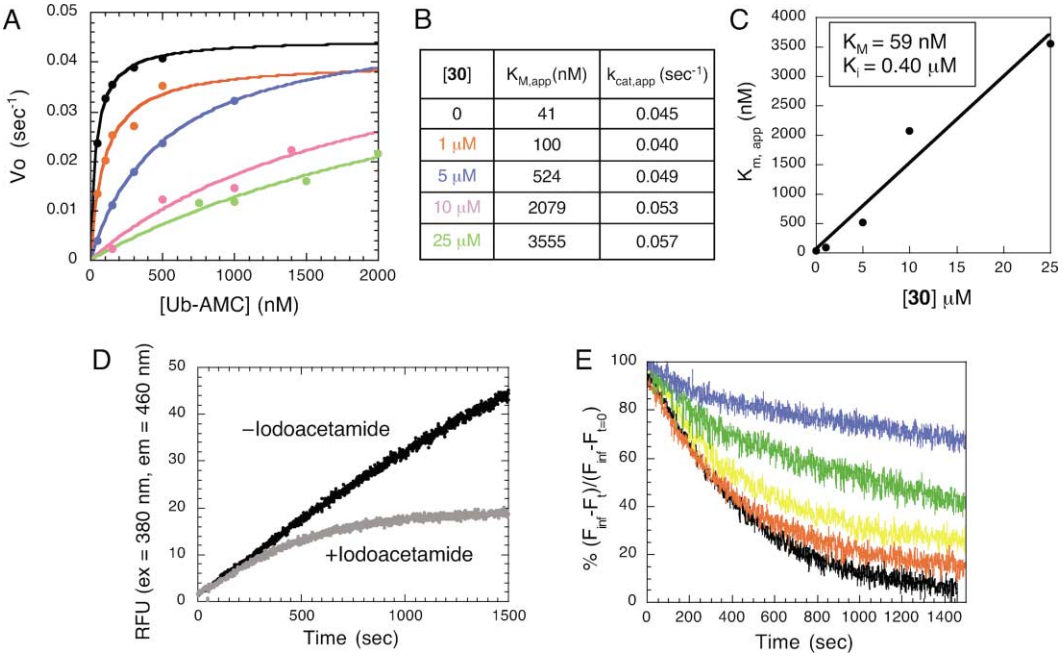

[30]	$K_{M,app}$(nM)	$k_{cat,app}$ (sec^{-1})
0	41	0.045
1 μM	100	0.040
5 μM	524	0.049
10 μM	2079	0.053
25 μM	3555	0.057

Figure 4. Compound 30 Is a Reversible Competitive Inhibitor

(A) Dependence of Vo/[E] on [Ub-AMC] at five fixed concentration of **30** (black, 0; red, 1 μM; blue, 5 μM; pink, 10 μM; green, 25 μM).

(B) Summary of $K_{M,app}$ and $k_{cat,app}$ values.

(C) Dependence of of $K_{M,app}$ on [**30**] yields K_M of 59 nM and K_i of 0.40 μM.

(D) Ub-AMC reaction progress curves in the presence or absence of iodoacetamide (20 mM).

(E) Normalized progress curves showing the amount of active UCH-L1 remaining in the reaction mixture in the presence of 20 mM iodoacetamide and various concentrations of **30** (black, 0; red, 500 nM; yellow, 1 μM; green, 3 μM; blue, 5 μM).

of H358 cells). The failure of the equipotent UCH-L1 inhibitor **30** to demonstrate significant proproliferative activity may be due to its inefficient transport into H1299 cells; in fact, both **30** and **52** increased proliferation of a UCH-L1-expressing neuroblastoma line (SH-SY5Y) (see Supplemental Data at http://www.chembiol.com/cgi/content/full/10/9/837/DC1). To test whether the observed pro-proliferative activity was the result of inhibition of UCH-L1, the H1299 line was stably transfected with a UCH-L1 RNAi vector to suppress UCH-L1 expression. The H1299 line was also stably transfected with a UCH-L1 expression vector to increase expression. In the three H1299 lines, the expression level of UCH-L1 inversely correlated with cell proliferation, in this case measured by the MTT assay (Figure 5D). This result is consistent with the notion that the effect of the small molecule inhibitors is mediated by UCH-L1 and that UCH-L1 activity opposes proliferation. The change in UCH-L1 expression level also resulted in a morphological change in the H1299 cells (Figures 5E–5G). An increasing level of UCH-L1 correlated with an increase in cell size and a morphology with more extended processes, two phenomena that also have been observed in an acute lymphoblastic leukemia cell line, Reh [33, 34]. Thus, in H1299 cells, UCH-L1 may affect the cell cycle and cell growth without affecting the cell viability.

Discussion

The neuronal enzyme UCH-L1 is implicated in PD and cancer, but the details of its role are unknown. These details are critical in order to determine whether UCH-L1 represents a viable drug target for either of these indications. As an alternative to treatment with small molecules, which most often are inhibitors, mouse models can be genetically manipulated to test the effect of protein expression level (decrease *and* increase) on a chosen phenotype. While a transgenic mouse that overexpresses UCH-L1 has not been reported, a mouse harboring a spontaneous deletion of a major portion of the UCH-L1 gene has been identified. Mice that are homozygous for the deletion (a model of the completely inhibited state) develop a neurodegenerative phenotype that is distinct from PD (gracile axonal dystrophy, gad) [8, 35–39]. Mice that are heterozygous for the deletion express a significantly reduced amount of UCH-L1 (~50%–80% of normal, a model of the partially inhibited state), yet are neurologically indistinguishable from the wild-type mice [8, 35–39]. Mice generated by crossing homozygous gad mice with UCH-L3 knockout mice exhibit a more severe neurodegenerative phenotype than the gad homozygotes (the UCH-L3 knockouts did not show any neurodegeneration) [8]. None of these mice have been used in studies of tumorogenesis or neuropathic pain, which have also been linked to UCH-L1 [40].

The chemical genetic approach to UCH-L1 inhibition described here identified a class of isatin O-acyl oxime derivatives that are reversible, active site-directed inhibitors and demonstrate good selectivity for UCH-L1 versus UCH-L3. We demonstrate that these inhibitors promote the growth of a lung tumor cell line, a result that

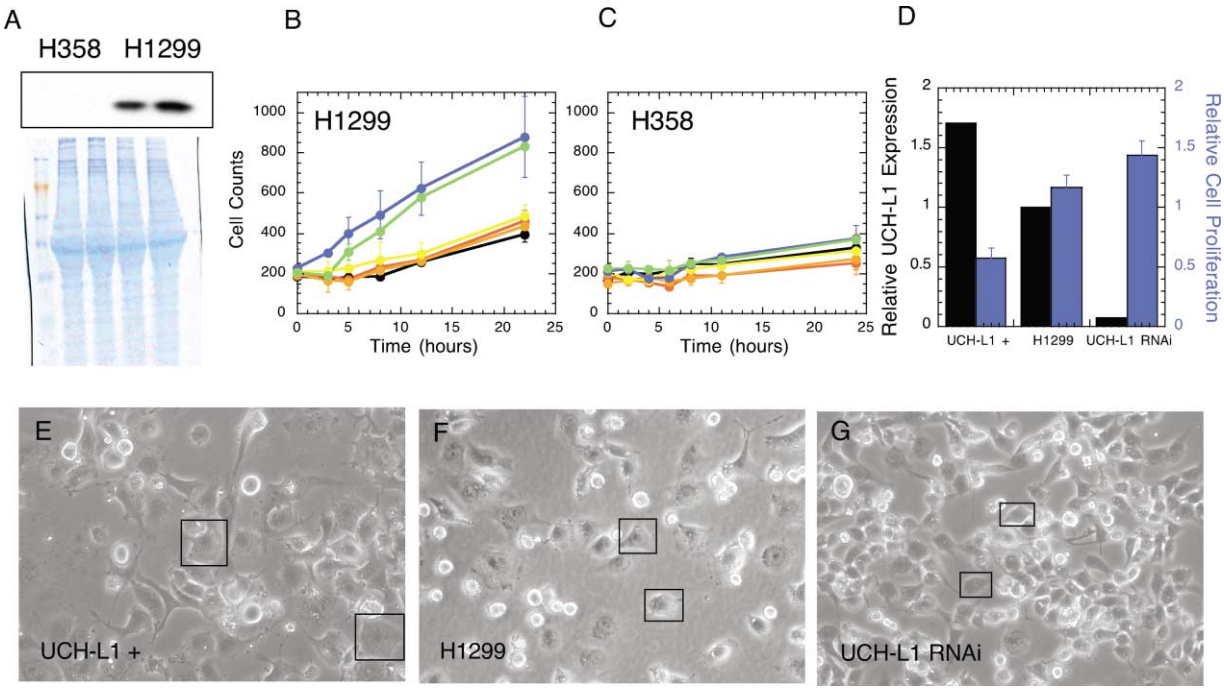

Figure 5. UCH-L1 Inhibition in Lung Cancer Cell Lines

(A) UCH-L1 (Western blot at top) is expressed in the H1299 cell line (two right lanes), but not the H358 line (two left lanes). The Coomassie-stained SDS-PAGE gel at bottom showed equal amounts of cell lysates were loaded.

(B and C) The H1299 (B) and H358 (C) cell lines showed a different sensitivity to small molecules (black, DMSO; red, **15**; orange, **24**; yellow, **30**; green, **50**; and blue, **52**).

(D) UCH-L1 expression and cell proliferation (MTT assay) are inversely correlated in H1299 UCH-L1+, H1299, and H1299 UCH-L1 RNAi cell lines.

(E–G) A more differentiated cell morphology and larger cell size are associated with increasing expression of UCH-L1 in H1299 cells.

is consistent with UCH-L1's antiproliferative effect observed upon modulation of UCH-L1 expression level. However, many questions remain to be answered. While promotion of UCH-L1 expression could slow tumor cell proliferation, the downstream effect of UCH-L1 activity on cell migration and invasion, for example, may be detrimental, as suggested by the positive correlation of UCH-L1 expression with tumor stage, T-status, and lower survival rate of the lung, colorectal, and pancreatic cancer patients [17, 19, 22, 41]. Furthermore, we have previously shown that UCH-L1 has two enzymatic activities, a weak hydrolase activity and a unique ligase activity [9]. It remains an open question as to which enzymatic activity (or combination thereof) is responsible for the reported antiproliferative effect in cancer cells. Using the similar approach, we hope to find small molecules that inhibit UCH-L1 ligase activity by disrupting UCH-L1 dimerization. These compounds will help to elucidate UCH-L1's roles in the diverse pathways that contribute to the pathogenesis of cancer and PD.

Significance

Ubiquitylation/deubiquitylation pathways are increasingly recognized as important in diverse cellular processes in addition to proteasome-dependent protein degradation. The abundant neuronal enzyme ubiquitin C-hydrolase-L1 (UCH-L1) is involved in the growth of some nonneuronal tumors, but it is not clear whether UCH-L1 expression drives tumor formation or is a response to tumor proliferation. To enable a chemical genetic approach to this question, we undertook a high-throughput screen of 42,000 drug-like compounds to identify UCH-L1 inhibitors. Hits from this screen were then modified to increase their potency toward UCH-L1 and their selectivity against UCH-L3. We report here the first class of small molecule UCH-L1 inhibitors. Treatment of lung tumor lines with these compounds indicated that UCH-L1 activity is antiproliferative and that its expression is probably induced as a response to tumor growth. These compounds will facilitate investigation of the role of UCH-L1 in Parkinson's disease, cancer, and neuropathic pain.

Experimental Procedures

Chemicals and Materials

All chemicals used in protein purification and enzymatic reactions were purchased from Sigma-Aldrich and used without purification. Protein purification columns were purchased from Amersham Pharmacia.

Proteins

Plasmids for prokaryotic expression of UCH-L1 and UCH-L3 were a gift from K. Wilkinson. Each plasmid was transformed into BL21(DE3) competent cells (Novagen). The transformed cells were grown on LB plate containing ampicillin overnight at 37°C. LB cultures (7 ml) containing 0.15 mg/l ampicillin were each inoculated with a single colony of transformed BL21(DE3) cell and shaken at

250 rpm and 37°C. The overnight cultures were used to inoculate 2 l of LB/ampicillin media for each enzyme expression. The cells were shaken at 250 rpm and at 37°C until OD of 0.5 at 600 nm was reached. IPTG (0.5 mM) was added to the cell culture to induce protein expression. After 2–3 hr of additional incubation/shaking at 37°C, cells were harvested by centrifugation at 8000 rpm for 10 min at 4°C. Cell pellets were resuspended in 100 ml of UCH protein buffer (50 mM Tris-HCl [pH 7.6], 0.5 mM EDTA, 1 mM DTT) in the presence of PMSF and then lysed using a Microfluidizer Processor (9000). Streptomycin sulfate was added (final 1% weight/volume) into each cell lysate and the mixtures were incubated on ice for 10 min prior to centrifugation at 10,000 rpm for 20 min at 4°C. The supernatant (30 ml for each run) was fractionated on HiTrap Q XL column (5 ml column volume) in UCH protein buffer with 0 to 600 mM NaCl gradient using AKTA FPLC (Amersham Pharmacia). UCH enzyme fractions were combined and dialyzed in UCH protein buffer overnight at 4°C. For UCH-L1 protein purification, the collected protein samples were furthered purified using a HiTrap Benzamidine column (1 ml column volume) in UCH protein buffer with 0 to 600 mM NaCl grandient. Instead of using a benzamidine column, UCH-L3 was subjected to gel filtration column purification using a HiLoad 16/60 Superdex 75 preparative grade gel filtration column equilibrated with UCH buffer. Fractions containing UCH enzymes were combined and dialyzed in UCH protein buffer overnight at 4°C. The proteins were aliquoted into small volume and stored at −80°C. SDS-PAGE showed that the proteins were >98% pure and protein concentrations were determined by amino acid analysis.

HTS for UCH-L1 Inhibitors

The compound library used for screening against UCH-L1 contained ~42,000 molecules purchased from Prestwick (Illkirch, France), Specs and Biospecs (CP Rijswijk, Netherlands), Bionet Research Ltd. (Cornwall, UK), Maybridge Plc. (Cornwall, UK), Cerep (Paris, France), Peakdale (High Peak, UK), and Chemical Diversity Labs, Inc. (San Diego, CA). The compound libraries were delivered predissolved in DMSO or in powdered form in 96-well tube racks. The powdered compounds were reconstituted in DMSO to 5 mg/ml. Four 96-well tube racks were combined into each 384-well master plate, via the quadrant mapping system. All compounds were stored at −20°C prior to use.

The HTS screen was performed on a Beckman Coulter Biomek FX liquid handling station integrated into a Saigian core system built around an ORCA robotic arm. This core system consists of a plate washer, plate shaker, temperature- and CO_2-controlled incubator, and plate carousel for storage. To start an assay, 0.5 μl of 5 mg/ml test compound (about 50 μM final reaction concentration) or DMSO control was aliquoted into each well. Both enzyme and substrate were prepared in UCH reaction buffer (50 mM Tris-HCl [pH 7.6], 0.5 mM EDTA, 5 mM DTT, and 0.5 mg/ml ovalbumin). 25 μl of 0.6 nM UCH-L1 was then added to each well except substrate control wells, followed by plate shaking for 45–60 s on an automatic shaker. The enzyme/compound mixture was incubated at room temperature for 30 min before 25 μl of 200 nM Ub-AMC (Boston Biochem, Cambridge, MA) was added to initiate the enzyme reaction. The reaction mixture (300 pM UCH-L1, 100 nM Ubiquitin-AMC with 2.5 μg test compound) was incubated at room temperature for 30 additional minutes prior to quenching the reaction by the addition of 10 μl 500 mM acetic acid per well. The fluorescence emission intensity was measured on a LJL Analyst using a coumarin filter set (ex = 365 nm, em = 450 nm) and was subtracted by the intrinsic compound fluorescence to reveal the enzyme activity. A DMSO control (0.5 μl of DMSO, 25 μl of UCH-L1, 25 μl of ubiquitin-AMC, 10 μl of acetic acid), enzyme control (25 μl of UCH-L1, 25 μl of buffer, 10 μl of acetic acid), substrate control (25 μl of buffer, 25 μl of ubiquitin-AMC, 10 μl of acetic acid), and inhibitor control (0.5 μl of ubiquitin aldehyde [100 nM stock], 25 μl of UCH-L1, 25 μl of ubiquitin-AMC, 10 μl of acetic acid) were also performed in each assay plate to ensure quality and reproducibility. Potential UCH-L1 inhibitors were selected if the compounds demonstrated greater than 60% inhibition compared to the controls. The UCH-L1 enzymatic reactions were manually repeated twice using the same protocol to confirm the results for the hit compounds from the primary robot-assisted screen.

Dose-Dependent Assays

Compounds that showed consistent activity toward UCH-L1 enzymatic activity through the primary and secondary screen were then tested in a dose-dependent assay, also using 384-well plates. UCH-L1/Ub-AMC reaction was performed with a series dilution of each compound (100 μM, 50 μM, 20 μM, 4 μM, 800 nM, 160 nM, 32 nM, 6.4 nM, 1.3 nM, and 260 pM). Compounds that did not exhibit dose-dependent activity toward UCH-L1 were eliminated from the candidate list.

Quenching of AMC Fluorophore with Each Inhibitor Compound

To eliminate a false positive due to fluorescence quenching of AMC amine by the test compound, a series of control experiments were performed in which 100 μM of each compound was incubated in a solution containing 100 nM AMC amine. Compounds that quenched AMC amine fluorescence were removed from the initial library.

IC_{50} Value Determinations

Various concentrations (100 μM to 50 nM) of compound dissolved in DMSO were each added to 2 ml of 1 nM UCH-L1 or 50 pM UCH-L3 in UCH reaction buffer and incubated at 25°C for 30 min. Ubiquitin C-terminal hydrolysis activity was initiated by adding 2 μl of 50 μM ubiquitin-AMC. The reactions were monitored at 25°C using a Hitachi F4500 fluorescence spectrophotometer. The AMC fluorophore was excited at 380 nm and the rates of release of free AMC were measured by monitoring the increase in fluorescence emission at 460 nm. The initial velocity *Vo* was measured for each reaction and plotted against compound concentrations in order to determine the IC_{50} values using GraFit V.5 software (Erithacus Software, UK).

K_i Value Determination for Compound 30

Various concentrations of compound **30** (0, 1 μM, 5 μM, 10 μM, and 25 μM) dissolved in DMSO were each added to 2 ml of 1 nM UCH-L1 in UCH reaction buffer and incubated at 25°C for 30 min. Ubiquitin C-terminal hydrolysis activity was initiated by adding various amounts of 100 μM ubiquitin-AMC stock solution to give a range of final concentrations between 10 nM and 2 μM. The reactions were monitored at 25°C using a Hitachi F4500 fluorescence spectrophotometer. The initial velocity *Vo* was measured for each reaction and plotted against Ub-AMC concentrations in order to determine the $K_{M,app}$ and $k_{cat,app}$. The K_M and K_i values were determined from the linear fit of $K_{M,app}$ versus [**30**].

Compound 30 Titration in UCH-L1/Iodoacetamide Reactions

UCH-L1 enzymatic activity in the presence or absence of iodoacetamide was monitored using Ub-AMC substrate in UCH reaction buffer. Iodoacetamide (20 mM) was added to the 5 nM UCH-L1 and 200 nM UbAMC reaction mixtures within 1 min after the reactions were started. To characterize the effect of **30** on UCH-L1 inactivation by iodoacetamide, various amounts (500 nM to 5 μM) of **30** were incubated with UCH-L1 for 5 min prior to the initiation of the Ub-AMC reaction followed by addition of iodoacetamide. The progress curves for the reactions containing iodoacetamide and/or **30** were normalized by the final AMC product fluorescence emission intensity $[(F_{infinite} - F_t)/(F_{infinite} - F_{t=0}) \times 100]$.

General Procedure for the Preparation of O-Acyloxime Isatins, Exemplified for 30 (LDN-57444)

To a solution of 5-chloroisatin (182 mg, 1.0 mmol) in anhydrous dimethylformamide (4 ml) was added sodium hydride (60 mg, 60% dispersion in mineral oil, 5 mmol) at 0°C under an argon atmosphere. The mixture was stirred at room temperature for 30 min before the addition of 2, 5-dichlorobenzyl chloride (240 mg, 1.0 mmol). The resulting mixture was stirred overnight. The reaction mixture was diluted with EtOAc (60 ml), washed with brine (10 ml), dried over anhydrous $MgSO_4$, filtered, and concentrated. The residue was purified by column chromatography on silica gel using hexane/ethyl acetate (2:1) as eluent to give N-(2, 5-dichlorobenzyl)-5-chloroisatin (204 mg, 60% yield) as a red solid. ^{1}H NMR (500 MHz, $CDCl_3$): δ 5.02 (s, 2H), 6.72 (d, 1H, J = 8.5 Hz), 7.18 (d, 1H, J = 2.5 Hz), 7.26 (dd, 1H, J = 2.5, 8.5 Hz), 7.38 (d, 1H, J = 8.5 Hz), 7.50 (dd, 1H, J = 2.5, 8.5 Hz), 7.64 (d, 1H, J = 2.5 Hz).

To a solution of N-(2, 5-dichlorobenzyl)-5-chloroisatin (34 mg, 0.1 mmol) in MeOH/THF (1:1, 2 ml) were added hydroxylamine hydrochloride (140 mg, 2.0 mmol) and sodium acetate (166 mg, 2.0 mmol). The mixture was stirred at room temperature overnight, then diluted with EtOAc (40 ml), washed with saturated $NaHCO_3$ (10 ml) and brine (10 ml), dried over anhydrous $MgSO_4$, filtered, and concentrated. The crude N-(2, 5-dichlorobenzyl)-5-chloroisatin oxime was used without further purification.

To a solution of the oxime ($\sim$0.1 mmol) in dry pyridine (2 ml) was added acetic anhydride (0.5 ml, mmol) at room temperature under an argon atmosphere. The mixture was stirred for 2 hr and then partitioned between ethyl acetate (30 ml) and 1 N HCl (10 ml). The organic layer was washed sequentially with 1N HCl (10 ml), saturated $NaHCO_3$ (5 ml), and brine (10 ml), dried over anhydrous $MgSO_4$, filtered, and concentrated. The product was purified by column chromatography on silica gel using hexane/ethyl acetate (2:1) to give **30** as a pale yellow solid (35 mg, 87% yield over two steps). mp 178°C–181°C; ^{1}H NMR (500 MHz, $CDCl_3$): δ 2.50 (s, 3H), 5.03 (s, 2H), 6.68 (d, 1H, J = 8.5 Hz), 7.12 (d, 1H, J = 2.5 Hz), 7.23 (dd, 1H, J = 2.5, 8.5 Hz), 7.36 (d, 1H, J = 8.5 Hz), 7.39 (dd, 1H, J = 2.0, 9.0 Hz), 8.05 (d, 1H, J = 2.0 Hz); ^{13}C NMR (100.5 MHz, $CDCl_3$): δ 19.72 (CH_3), 41.43 (CH_2), 111.10 (CH), 116.12 (C), 128.23 (CH), 129.55 (C), 129.68 (CH), 129.78 (CH), 131.26 (CH), 131.33 (C), 133.81 (2$\times$C), 134.64 (CH), 142.98 (C), 147.06 (C), 162.57 (C), 168.32 (C); FT-IR (KBr, ν_{max}, cm^{-1}): 3444w, 3070w, 2924m, 2852w, 1785s, 1731s, 1608s, 1471s, 1442m, 1338m, 1170s, 928s, 917s, 826m; Elemental Analysis calculated for $C_{17}H_{11}Cl_3N_2O_3$: C, 51.35; H, 2.79; N, 7.04; found: C, 51.31; H, 3.19; N, 6.84.

Cell-Base O-Acyl Oxime Compound Assays

H1299 and H358 non-small cell lung cancer cell lines were purchased from American Type Culture Collection (ATCC) and were maintained in RPMI medium (ATCC) containing 10% fetal bovine serum. Cells were cultured at 37°C for 24 hr prior to treatments with the 5 μM **15**, **24**, **30**, **50**, **52**, or DMSO. Cells were counted under light microscope at each time point.

Transfection of H1299 Cells with UCH-L1 Expressing and RNAi Vectors

UCH-L1 was cloned into pcDNA3.1 (Invitrogen) with restriction enzymes Xho I and Hind III. UCH-L1 RNAi vector was constructed by inserting synthetic DNA (GATCCCCCCCGAGATGCTGAACAAAGTT CAAGAGACTTTGTTCAGCATCTCGGGTTTTTGGAAA annealed with its complementary strand) into pSUPER.retro (OligoEngine, Seattle, WA) between Hind III and EcoR I restriction sites. Both vectors were transfected into H1299 using Lipofectamine 2000 (Invitrogen). UCH-L1 expression levels were analyzed by Western blots and normalized by the total protein quantified by Coomassie staining. The proliferation rate of each cell line was measured using standard MTT assay.

Supplemental Data

Supplemental Data is available at http://www.chembiol.com/cgi/content/full/10/9/837/DC1.

Acknowledgments

This work was supported by funding from the Harvard Center for Neurodegeneration and Repair (HCNR), a Morris K. Udall Parkinson's Disease Research Center of Excellence grant (NS38375), the James K. Warsaw Foundation to Cure Parkinson's Disease, and the Kinetics Foundation. Y.L. is an NIH postdoctoral fellow and was previously supported by the Harvard Molecular Biology of Neurodegeneration Training Program. H.A.L. was a postdoctoral fellow of the Laboratory for Drug Discovery in Neurodegeneration, a core component of the HCNR.

Received: May 6, 2003
Revised: July 16, 2003
Accepted: July 21, 2003
Published: September 19, 2003

References

1. Wilkinson, K.D., Lee, K.M., Deshpande, S., Duerksen-Hughes, P., Boss, J.M., and Pohl, J. (1989). The neuron-specific protein PGP 9.5 is a ubiquitin carboxyl-terminal hydrolase. Science *246*, 670–673.
2. Leroy, E., Boyer, R., Auburger, G., Leube, B., Ulm, G., Mezey, E., Harta, G., Brownstein, M.J., Jonnalagada, S., Chernova, T., et al. (1998). The ubiquitin pathway in Parkinson's disease. Nature *395*, 451–452.
3. Larsen, C.N., Price, J.S., and Wilkinson, K.D. (1996). Substrate binding and catalysis by ubiquitin C-terminal hydrolases: identification of two active site residues. Biochemistry *35*, 6735–6744.
4. Larsen, C.N., Krantz, B.A., and Wilkinson, K.D. (1998). Substrate specificity of deubiquitinating enzymes: ubiquitin C-terminal hydrolases. Biochemistry *37*, 3358–3368.
5. Wilkinson, K.D. (1997). Regulation of ubiquitin-dependent processes by deubiquitinating enzymes. FASEB J. *11*, 1245–1256.
6. Dang, L.C., Melandri, F.D., and Stein, R.L. (1998). Kinetic and mechanistic studies on the hydrolysis of ubiquitin C-terminal 7-amido-4-methylcoumarin by deubiquitinating enzymes. Biochemistry *37*, 1868–1879.
7. Chung, C.H., and Baek, S.H. (1999). Deubiquitinating enzymes: their diversity and emerging roles. Biochem. Biophys. Res. Commun. *266*, 633–640.
8. Kurihara, L.J., Kikuchi, T., Wada, K., and Tilghman, S.M. (2001). Loss of Uch-L1 and Uch-L3 leads to neurodegeneration, posterior paralysis and dysphagia. Hum. Mol. Genet. *10*, 1963–1970.
9. Liu, Y., Fallon, L., Lashuel, H.A., Liu, Z., and Lansbury, P.T., Jr. (2002). The UCH-L1 gene encodes two opposing enzymatic activities that affect alpha-synuclein degradation and Parkinson's disease susceptibility. Cell *111*, 209–218.
10. Maraganore, D.M., Farrer, M.J., Hardy, J.A., Lincoln, S.J., McDonnell, S.K., and Rocca, W.A. (1999). Case-control study of the ubiquitin carboxy-terminal hydrolase L1 gene in Parkinson's disease. Neurology *53*, 1858–1860.
11. Levecque, C., Destee, A., Mouroux, V., Becquet, E., Defebvre, L., Amouyel, P., and Chartier-Harlin, M.C. (2001). No genetic association of the ubiquitin carboxy-terminal hydrolase-L1 gene S18Y polymorphism with familial Parkinson's disease. J. Neural Transm. *108*, 979–984.
12. Satoh, J.I., and Kuroda, Y. (2001). Ubiquitin C-terminal hydrolase-L1 (PGP9.5) expression in human neural cell lines following induction of neuronal differentiation and exposure to cytokines, neurotrophic factors or heat stress. Neuropathol. Appl. Neurobiol. *27*, 95–104.
13. Momose, Y., Murata, M., Kobayashi, K., Tachikawa, M., Nakabayashi, Y., Kanazawa, I., and Toda, T. (2002). Association studies of multiple candidate genes for Parkinson's disease using single nucleotide polymorphisms. Ann. Neurol. *51*, 133–136.
14. Wang, J., Zhao, C.Y., Si, Y.M., Liu, Z.L., Chen, B., and Yu, L. (2002). ACT and UCH-L1 polymorphisms in Parkinson's disease and age of onset. Mov. Disord. *17*, 767–771.
15. Elbaz, A., Levecque, C., Clavel, J., Vidal, J.S., Richard, F., Correze, J.R., Delemotte, B., Amouyel, P., Alperovitch, A., Chartier-Harlin, M.C., et al. (2003). S18Y polymorphism in the UCH-L1 gene and Parkinson's disease: evidence for an age-dependent relationship. Mov. Disord. *18*, 130–137.
16. Caballero, O.L., Resto, V., Patturajan, M., Meerzaman, D., Guo, M.Z., Engles, J., Yochem, R., Ratovitski, E., Sidransky, D., and Jen, J. (2002). Interaction and colocalization of PGP9.5 with JAB1 and p27(Kip1). Oncogene *21*, 3003–3010.
17. Sasaki, H., Yukiue, H., Moriyama, S., Kobayashi, Y., Nakashima, Y., Kaji, M., Fukai, I., Kiriyama, M., Yamakawa, Y., and Fujii, Y. (2001). Expression of the protein gene product 9.5, PGP9.5, is correlated with T-status in non-small cell lung cancer. Jpn. J. Clin. Oncol. *31*, 532–535.
18. Bittencourt Rosas, S.L., Caballero, O.L., Dong, S.M., da Costa Carvalho Mda, G., Sidransky, D., and Jen, J. (2001). Methylation status in the promoter region of the human PGP9.5 gene in cancer and normal tissues. Cancer Lett. *170*, 73–79.
19. Hibi, K., Westra, W.H., Borges, M., Goodman, S., Sidransky, D., and Jen, J. (1999). PGP9.5 as a candidate tumor marker for non-small-cell lung cancer. Am. J. Pathol. *155*, 711–715.

20. Hibi, K., Liu, Q., Beaudry, G.A., Madden, S.L., Westra, W.H., Wehage, S.L., Yang, S.C., Heitmiller, R.F., Bertelsen, A.H., Sidransky, D., et al. (1998). Serial analysis of gene expression in non-small cell lung cancer. Cancer Res. *58*, 5690–5694.
21. Sunday, M.E., Willett, C.G., Graham, S.A., Oreffo, V.I., Linnoila, R.I., and Witschi, H. (1995). Histochemical characterization of non-neuroendocrine tumors and neuroendocrine cell hyperplasia induced in hamster lung by 4-(methylnitrosamino)-1-(3-pyridyl)-1-butanone with or without hyperoxia. Am. J. Pathol. *147*, 740–752.
22. Yamazaki, T., Hibi, K., Takase, T., Tezel, E., Nakayama, H., Kasai, Y., Ito, K., Akiyama, S., Nagasaka, T., and Nakao, A. (2002). PGP9.5 as a marker for invasive colorectal cancer. Clin. Cancer Res. *8*, 192–195.
23. Grozinger, C.M., and Schreiber, S.L. (2002). Deacetylase enzymes: biological functions and the use of small-molecule inhibitors. Chem. Biol. *9*, 3–16.
24. Haggarty, S.J., Mayer, T.U., Miyamoto, D.T., Fathi, R., King, R.W., Mitchison, T.J., and Schreiber, S.L. (2000). Dissecting cellular processes using small molecules: identification of colchicine-like, taxol-like and other small molecules that perturb mitosis. Chem. Biol. *7*, 275–286.
25. Johnston, S.C., Riddle, S.M., Cohen, R.E., and Hill, C.P. (1999). Structural basis for the specificity of ubiquitin C-terminal hydrolases. EMBO J. *18*, 3877–3887.
26. Melandri, F., Grenier, L., Plamondon, L., Huskey, W.P., and Stein, R.L. (1996). Kinetic studies on the inhibition of isopeptidase T by ubiquitin aldehyde. Biochemistry *35*, 12893–12900.
27. Zhang, J.H., Chung, T.D., and Oldenburg, K.R. (1999). A simple statistical parameter for use in evaluation and validation of high throughput screening assays. J. Biomol. Screen. *4*, 67–73.
28. Lipinski, C.A., Lombardo, F., Dominy, B.W., and Feeney, P.J. (2001). Experimental and computational approaches to estimate solubility and permeability in drug discovery and development settings. Adv. Drug Deliv. Rev. *46*, 3–26.
29. Gaeta, F., Galan, A.A., and Kraynack, E.A. (December 1999). Telomerase inhibitors. WO 99/65875.
30. Jensen, B.S., Jørgensen, T.D., Ahring, P.K., Christophersen, P., Strøbæk, D., Teuber, L., and Olesen, S.P. (June 2000). Use of isatine derivatives as Ion channel activating agents. WO 00/33834.
31. Wätjen, F., Drejer, J., and Jensen, L.H. (March 1993). Isatine derivatives, their preparation and use. U.S. patent 5,198,461.
32. Salituro, F.G., Bemis, G.W., Wilke, S., Green, J., Cao, J., Gao, H., and Harrington, E.M. (November 2000). Inhibitors of c-Jun N-terminal kinases (JNK). WO 00/64872.
33. Al-Katib, A.M., Mohammad, R.M., Maki, A., and Smith, M.R. (1995). Induced expression of a ubiquitin COOH-terminal hydrolase in acute lymphoblastic leukemia. Cell Growth Differ. *6*, 211–217.
34. Maki, A., Mohammad, R.M., Smith, M., and Al-Katib, A. (1996). Role of ubiquitin carboxyl terminal hydrolase in the differentiation of human acute lymphoblastic leukemia cell line, Reh. Differentiation *60*, 59–66.
35. Miura, H., Oda, K., Endo, C., Yamazaki, K., Shibasaki, H., and Kikuchi, T. (1993). Progressive degeneration of motor nerve terminals in GAD mutant mouse with hereditary sensory axonopathy. Neuropathol. Appl. Neurobiol. *19*, 41–51.
36. Mukoyama, M., Yamazaki, K., Kikuchi, T., and Tomita, T. (1989). Neuropathology of gracile axonal dystrophy (GAD) mouse. An animal model of central distal axonopathy in primary sensory neurons. Acta Neuropathol. *79*, 294–299.
37. Oda, K., Yamazaki, K., Miura, H., Shibasaki, H., and Kikuchi, T. (1992). Dying back type axonal degeneration of sensory nerve terminals in muscle spindles of the gracile axonal dystrophy (GAD) mutant mouse. Neuropathol. Appl. Neurobiol. *18*, 265–281.
38. Saigoh, K., Wang, Y.L., Suh, J.G., Yamanishi, T., Sakai, Y., Kiyosawa, H., Harada, T., Ichihara, N., Wakana, S., Kikuchi, T., et al. (1999). Intragenic deletion in the gene encoding ubiquitin carboxy-terminal hydrolase in gad mice. Nat. Genet. *23*, 47–51.
39. Wu, J., Ichihara, N., Chui, D.H., Yamazaki, K., and Kikuchi, T. (1995). Ubiquitin immunoreactivity in the central nervous system of gracile axonal dystrophy (GAD) mouse. No To Shinkei *47*, 881–885.
40. Moss, A., Blackburn-Munro, G., Garry, E.M., Blakemore, J.A., Dickinson, T., Rosie, R., Mitchell, R., and Fleetwood-Walker, S.M. (2002). A role of the ubiquitin-proteasome system in neuropathic pain. J. Neurosci. *22*, 1363–1372.
41. Tezel, E., Hibi, K., Nagasaka, T., and Nakao, A. (2000). PGP9.5 as a prognostic factor in pancreatic cancer. Clin. Cancer Res. *6*, 4764–4767.